

## CHAPTER IV

### SYNTHESIS AND CHARACTERIZATION OF TiO<sub>2</sub>/CdSe PHOTOANODE AND ITS APPLICATION FOR SOLAR CELL

Sr. No.	TITLE	Page No.
<b>4.1</b>	<b>Introduction</b>	69
<b>4.2</b>	<b>Experimental set up</b>	70
<b>4.3</b>	<b>Experimental details</b>	70
	4.3.1 Chemicals	70
	4.3.2 Substrate cleaning	71
	4.3.3 Solution preparation	71
<b>4.4</b>	<b>Deposition of TiO<sub>2</sub> on FTO</b>	72
<b>4.5</b>	<b>Deposition of CdSe nanoparticles thin layer on FTO/TiO<sub>2</sub> surface</b>	72
<b>4.6</b>	<b>Results and discussion</b>	74
	4.6.1 Characterization techniques	74
	4.6.2 Structural studies	74
	4.6.3 Optical absorption studies	75
	4.6.4 Surface morphological studies	76
	4.6.5 Size, shape, structure and elemental confirmation	77
	4.6.6 Device fabrication and testing	78
<b>4.7</b>	<b>Conclusions</b>	82

## Overview

This chapter includes three sections. First section describes the synthesis of layer heterostructure by using low cost wet chemical synthesis route. Here, we used spin coating technique for the synthesis of porous TiO<sub>2</sub> nanostructured and chemical bath deposition (CBD) technique for the synthesis of CdSe nanoparticles without using linker or ligand molecules. The particle sizes of the CdSe nanoparticles in ETA layer can be anchor by varying deposition time. While second section, includes characterizations of layer heterostructures by using different characterization techniques (i.e structural, optical, surface morphological and elemental). Finally, sandwich type solar cell device were constructed by using synthesized layer heterostructure as a photoanode, polysulphide as a liquid electrolyte and platinum as a back contact. The photovoltaic characteristics of all constructed device were measured in dark and light.

### 4.1. Introduction

This chapter describes the synthesis, characterization of TiO<sub>2</sub>/CdSe layer heterostructure and its application for solar cell device. The spin coating and chemical bath deposition (CBD) techniques have been used for the deposition of respective layers on the fluorine doped tin oxide (FTO) coated glass substrate.

The general introduction about spin coating technique has been explained in section 3.1 (chapter-III). While, the chemical bath deposition (CBD) technique is based on the principle of solubility product and ionic product. Where, cationic and anionic solutions are mixed together and if ionic product exceeds or become equal to the solubility product, precipitation occurs as ions combine on the substrate and in the solution to form nuclei. In this reaction, the basic building blocks are ions instead of atoms; hence reaction can be controlled at ionic layer by homogeneous precipitation. Till today, various reports are available for the deposition of various metal oxides and metal chalcogenides semiconducting material and some review articles shows the necessity and working principle of CBD [125-130]. The concentration, pH, temperature, deposition time plays crucial role in film formation. This technique widely used for the deposition of various nanostructured thin film including quantum dots (particle size < 10nm) onto the various substrates. The several preparative parameters are playing vital role in the chemical reaction. These include pH,

concentration, complexing agent, and deposition time are briefly explained in section 2.3.3 (chapter II).

The present chapter deals with the preparation of layer nanostructure between TiO<sub>2</sub> and CdSe by using spin coating and CBD technique sequentially on the FTO coated glass substrate. Finally, structural, surface morphological, elemental and photovoltaic parameters in dark under illumination of a simulated 50 mW/cm<sup>2</sup> light were studied and results are discussed herein.

## 4.2. Experimental set up

The desired device has the structure FTO/TiO<sub>2</sub>/CdSe/electrolyte/ platinum coated FTO as a back contact, which is shown in figure 4.2 (A). The schematic representation for the synthesis of TiO<sub>2</sub> on FTO is shown in figure 3.2(B) (chapter III) and sensitizer nanoparticles layer on FTO/TiO<sub>2</sub> at room temperature by using linker free wet chemical approach is shown in figure 2.3.3 (chapter II). The detailed experimental procedures for the deposition of layer heterostructure are explained in section 4.4 for TiO<sub>2</sub> and in section 4.5 for CdSe.

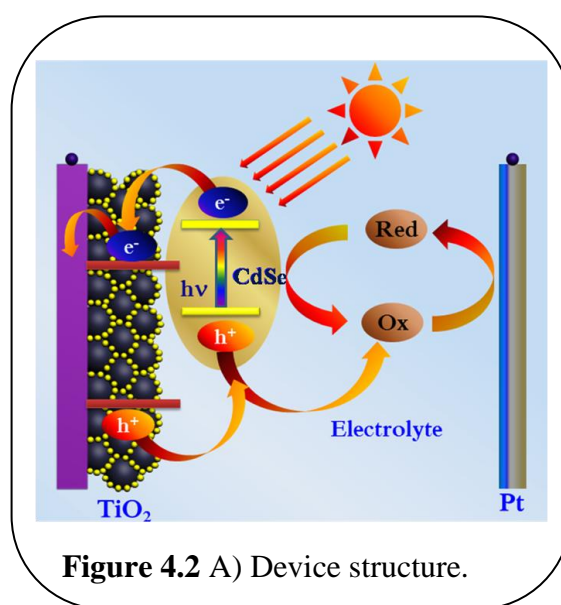


Figure 4.2 A) Device structure.

## 4.3. Experimental details

### 4.3.1. Chemicals

The chemicals include P-25 TiO<sub>2</sub> (Degussa, Germany), Ethanol absolute (Merck, Germany), acetyl acetone AR (Sigma Aldrich, Germany), titanium isopropoxide (Himedia, India), cadmium acetate, sodium sulphide AR, sodium hydroxide AR, Se metal granules, sodium sulphate and sulphur powder (Loba Chemie, India). These were purchased and used without any purification treatment. The preparative parameters were optimized to get desired FTO/TiO<sub>2</sub>/CdSe layer nanostructured for solar cell application. Detailed about substrate cleaning prior to the deposition, solution preparation and other parameters are discussed below.

### 4.3.2. Substrate cleaning

The 1 X 1 inch dimensions of FTO glass have been used as substrate for the sequential deposition of the TiO<sub>2</sub> and CdSe. The substrates cleaning process were explained in section 3.3.2 (chapter-III).

### 4.3.3. Solution preparation

The TiO<sub>2</sub> films were deposited by using spin coating technique by preparing TiO<sub>2</sub> gel. The preparation of TiO<sub>2</sub> gel was explained in section 3.3.3 of chapter-III.

The second layer of a CdSe was deposited by using chemical bath deposition (CBD). The 0.1 mM cationic solution was prepared into 50 ml of double distilled water and resultant solution having pH 7.

While anionic solution, sodium selenosulphate was prepared by reflux method using the following procedure:

1. Distilled water of 100 ml was taken.
2. Dissolved 10 gm of Na<sub>2</sub>SO<sub>3</sub> in water. If the pH of resultant solution is not ~9 then adjusted by using NaOH and heated upto 80 degree for 60 min.
3. 0.4 gm of Se powder added in heated water
4. Constant heating and stirring was done upto 8 hours.

The resultant solution having 0.01 M was obtained and then dilutes the solution by adding double distilled water (1:100 volume ratios) and solution having pH 8.

**Table 3.1** Preparative parameters for the deposition of TiO<sub>2</sub>/CdSe structure on FTO

Parameter	Precursors		
	TiO <sub>2</sub>	CdSe	
		Cationic	Anionic
Source	The TiO <sub>2</sub> gel was prepared by mixing in a proportion of 2 gm P-25 TiO <sub>2</sub> and 10 ml solvent containing mixture of acetyl acetone, ethanol and titanium isopropoxide.	Cadmium acetate	Sodium selenosulphate
Concentration (mM/L)		0.1	0.1
pH (~)		7	8
Temperature (°C)		27	27

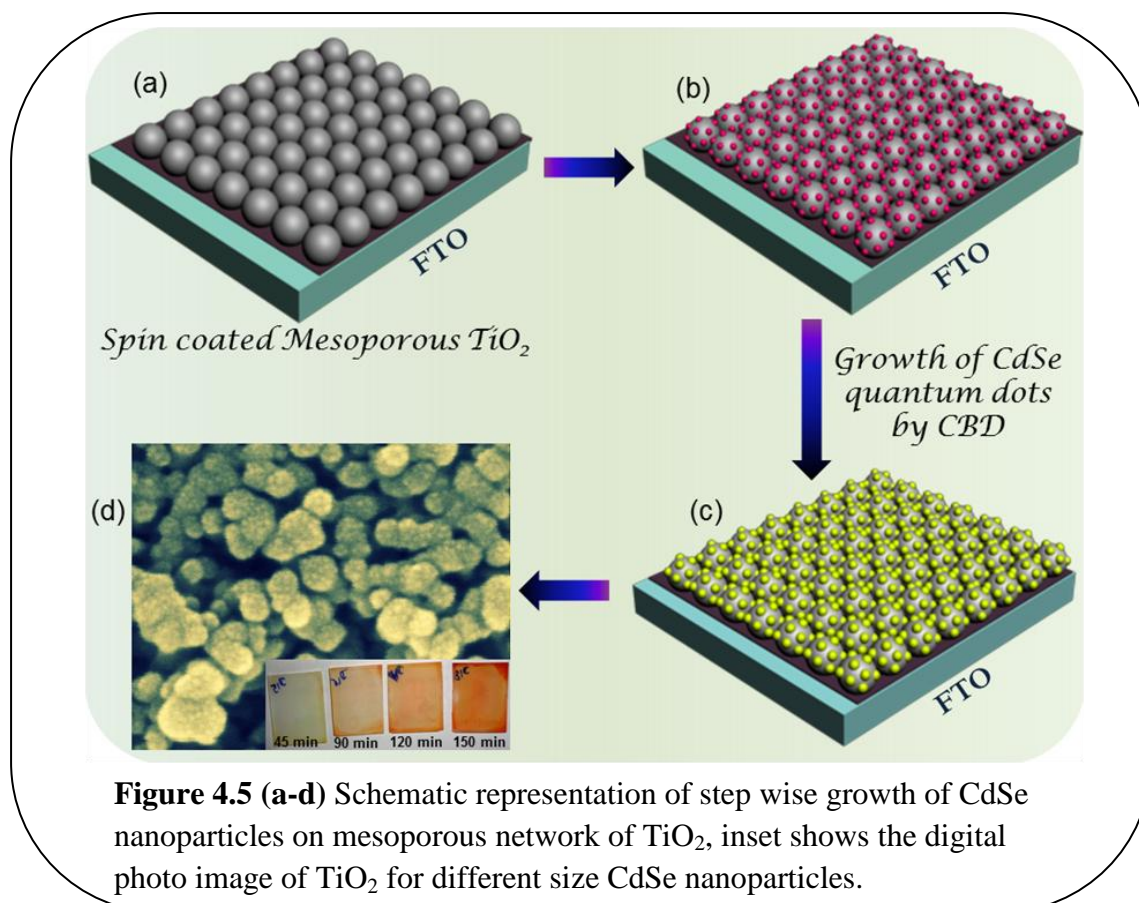
The table 3.1 summarizes parameters for the preparation of precursor solutions used for the sequential deposition of TiO<sub>2</sub> and CdSe on FTO and the steps involved in the synthesis are described in section 4.4 and 4.5.

#### 4.4. Deposition of TiO<sub>2</sub> on FTO

The spin coating technique has been used to coat porous TiO<sub>2</sub> nanostructured film on FTO (size: 1 X 1 inch) surface. The detailed deposition procedure is explained in section 3.4 (chapter-III).

#### 4.5. Deposition of CdSe nanoparticles layer on FTO/TiO<sub>2</sub> surface

Chemical bath deposition (CBD) technique was used to deposit the different size CdSe nanoparticles on the surface of mesoporous TiO<sub>2</sub> films. Where, cadmium acetate [Cd(CH<sub>3</sub>COO)<sub>2</sub>] complexes with ammonia was used as a cationic source; and sodium selenosulphate (Na<sub>2</sub>SeSO<sub>3</sub>) was used as an anionic source. Mesoporous TiO<sub>2</sub> films were immersed in (0.25 mM) cadmium acetate solution at room temperature (27°C) with constant stirring for 15 min. This is responsible for the chemical attachment of Cd<sup>2+</sup> ions on the TiO<sub>2</sub> surface of mesoporous film. The substrates were taken out, rinsed smoothly with double distilled water and transferred quickly in 0.1 mM cadmium acetate solution, then, followed by drop-wise addition (0.5 ml per min.) of (0.1 mM) sodium selenosulphate with constant and slow stirring. The drop wise addition of low concentrated selenium ions precursor solution react slowly Se<sup>2-</sup> with pre-adsorbed Cd<sup>2+</sup> ions on TiO<sub>2</sub> electrode as well as Cd<sup>2+</sup> ions in the bath and resulted



into CdSe nanoparticles. These nanoparticles attached on the surface of TiO<sub>2</sub> without use of bifunctional linker. The substrates were taken out with specific time intervals as 45, 90, 120 and 150 min. from the bath. This consecutive deposition of film consisting of CdSe nanoparticles on the surface of TiO<sub>2</sub> was accomplished by a sequence of color changes visible to naked eyes; it may be due to the quantum size effect. The schematic representation of step-wise growth of CdSe on mesoporous TiO<sub>2</sub> by CBD are illustrated in figure 4.5 (a-d). The inset of figure 4.5 (d) shows digital photo image of CdSe coated TiO<sub>2</sub> thin films at different deposition time. The synthesis of CdSe nanoparticles layer onto TiO<sub>2</sub> is given in chart 4.1.

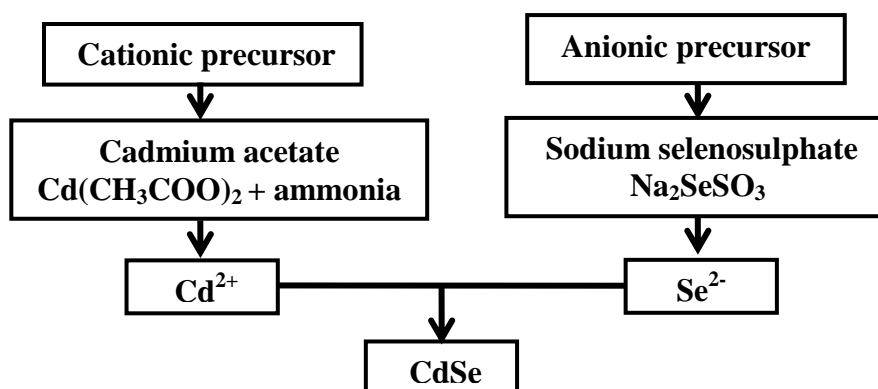
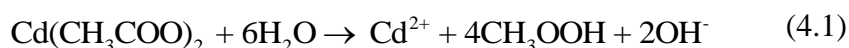


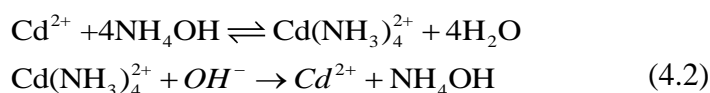
**Chart 4.1** Flowchart summarize the deposition process of CdSe by CBD technique

### Reaction mechanism

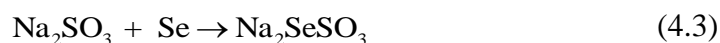
1. The 0.1 mM cationic solution of cadmium acetate was prepared into 50 ml of double distilled water and the resultant solution having pH 7.



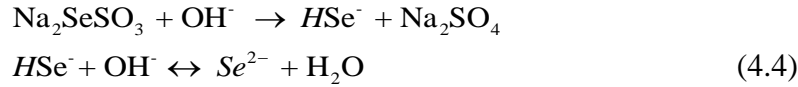
1. The addition of liquor ammonia in cationic solution forms a complex with Cd<sup>2+</sup> ions. Which slowly release Cd<sup>2+</sup> ions in the reaction bath and reaction mechanism is as shown below.



2. The 0.01 M anionic solution of sodium selenosulphate was prepared by reflux system then dilutes the solution by adding double distilled water (1:100 volume ratios) and resultant solution having 0.1 mM concentration and pH ~8.



- Anionic solution of sodium selenosulphate release Se<sup>2-</sup> ion in chemical bath, the reaction mechanism is shown as following



- The reaction bath the cationic react with anion and attached on the surface of TiO<sub>2</sub> and simplified version of reaction kinetics is as follow



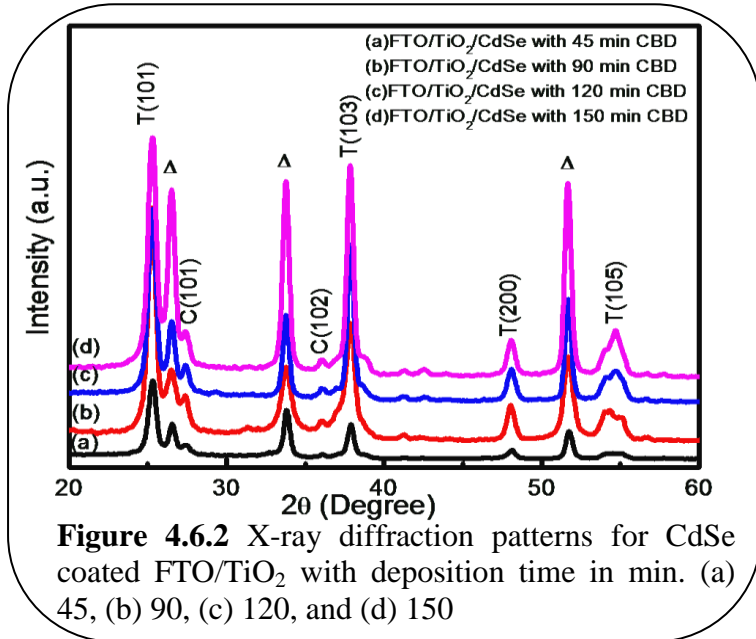
## 4.6. Results and discussion

### 4.6.1 Characterization techniques

The tools of characterization techniques are discussed in section 3.6.1 of chapter-III.

### 4.6.2 Structural studies

The diffraction patterns were recorded in the range of 20° to 60° for FTO, FTO/TiO<sub>2</sub> and CdSe coated on FTO/TiO<sub>2</sub> for different deposition time. The XRD pattern of FTO and FTO/TiO<sub>2</sub> electrodes explained in detailed in section 3.6.2 and illustrated in figure 3.6.2



(I) of chapter-III. The figure 4.6.2 (a-d) shows, XRD patterns of TiO<sub>2</sub>/CdSe heterostructure films synthesized at different CBD deposition time on FTO. In the diffraction patterns, the most intense peak observed at 2θ=25.3° assigned to (101) plane, which is attributed to anatase phase with tetragonal crystal structure of TiO<sub>2</sub> (JCPDS card no. 84-1285 and 21-1272). While, other small diffraction peaks appeared at 2θ= 37.81°, 47.99° and 54.6° stands for respective (103), (200) and (105) planes of the same phase and denoted by symbol (T). Two tiny peaks appeared along (101) and (102) planes as shown in Figure 4.6.2 (a-d) are composed of hexagonal crystal structure of CdSe (JCPDS card 77-0021) denoted by symbol (C). With

increasing CdSe deposition time peak intensity also increases. The additional peaks denoted by symbol ( $\Delta$ ) are for the FTO substrate. An average crystallite size of mesoporous TiO<sub>2</sub> for (101) plane and CdSe for (102) plane is calculated by using Debye-Scherrer's formula (equation 3.4 of chapter-III) and it is found to be 26 nm for TiO<sub>2</sub> and 6.9, 10.7, 13.6 and 20.6 nm, respectively for CdSe with increasing deposition time with correction factor of  $\pm 10\%$ .

#### 4.6.3 Optical absorption studies

The effect of coating of the CdSe ETA layer consisting of nanoparticles onto TiO<sub>2</sub>; on the optical properties of electrode was studied by using UV-Vis spectroscopy.

The absorbance spectra were recorded in 300 to 900 nm wavelength region of light. An absorption spectra of bare TiO<sub>2</sub> and four

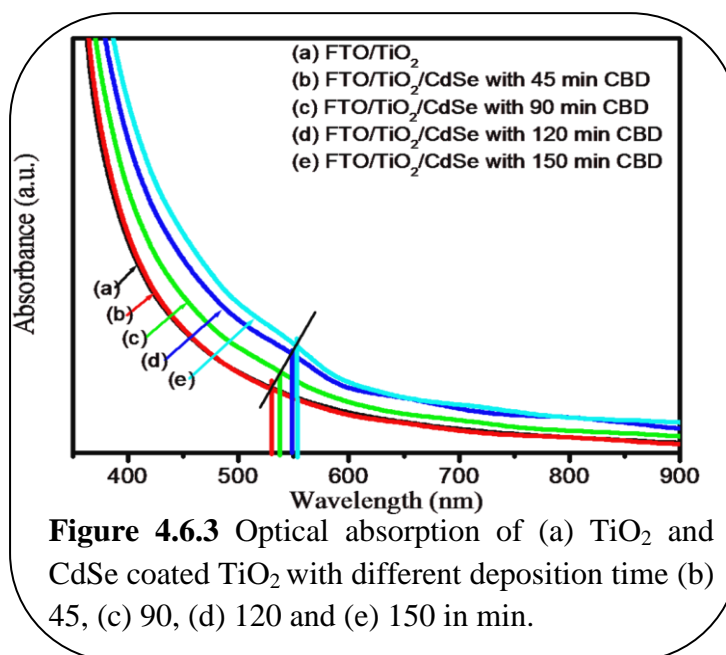
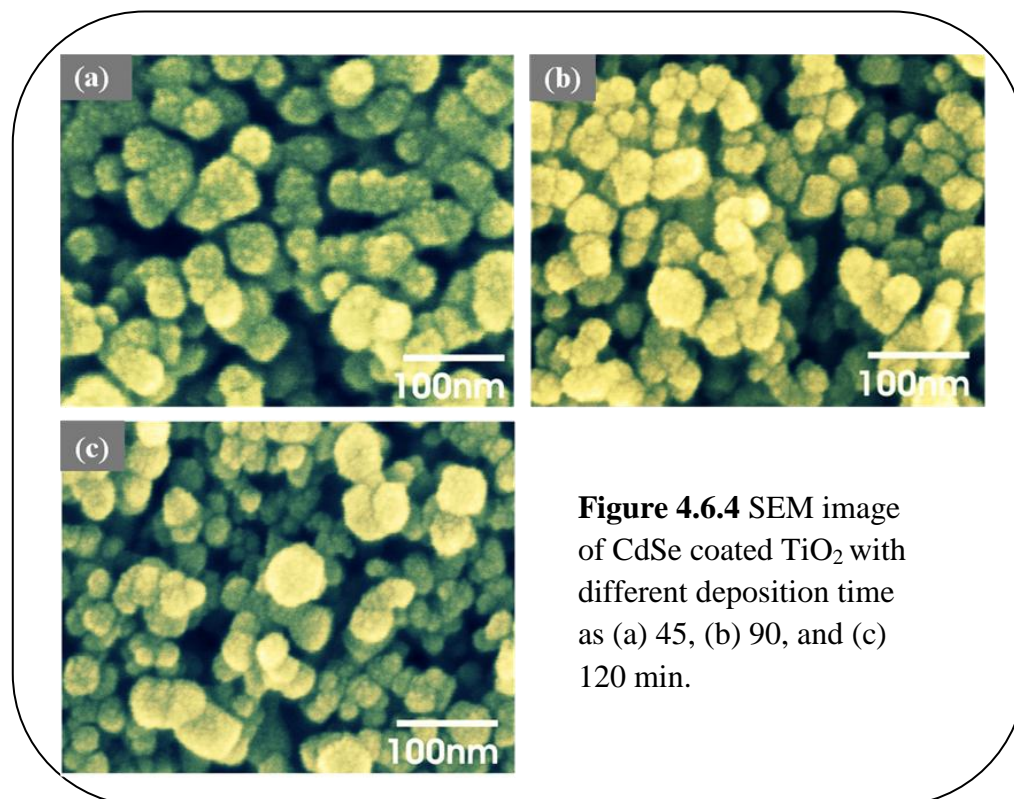


**Figure 4.6.3** Optical absorption of (a) TiO<sub>2</sub> and CdSe coated TiO<sub>2</sub> with different deposition time (b) 45, (c) 90, (d) 120 and (e) 150 in min.

different-sized CdSe nanoparticles coated TiO<sub>2</sub> network are illustrated in figure 4.6.3 (a-e), whereas FTO as a reference. The absorption spectrum of bare TiO<sub>2</sub> film were compared with CdSe coated TiO<sub>2</sub> at different CBD deposition time and these films shows, the diminutive absorption peaks at 535, 542, 548, 551 nm for 45, 90, 120 and 150 min depositions, respectively which are close to the band gap of CdSe as 2.31, 2.28, 2.26 and 2.25eV respectively. Band gap calculation was done as reported by Loef et al and Lee et al respectively [151a, 151b]. Because of the small electron effective mass ( $m_e = 0.13 m_o$ ) versus the significantly larger hole mass ( $m_h = 1.14 m_o$ ), the absorption onset is slowly shifted towards the longer wavelength region, known as red-shift compared to bulk band gap of CdSe (712 nm). This result confirms the size dependent properties of CdSe nanoparticles. Since the particle size of CdSe increases with respect to increase in deposition time, there is an escalation in the grain size, which results in the decrease in band gap. As a result, the excitation of electrons from valence band to conduction band requires lower energy, which results in the red-shift in UV-Vis absorption spectra. These results indicate that increase in agglomeration of

CdSe nanoparticles are incorporated on porous TiO<sub>2</sub> with increase in the CBD deposition time. Hence, there is increase in the sizes of the CdSe nanoparticles. The CBD technique is proficient to fill up the CdSe on the unfilled sites of mesoporous TiO<sub>2</sub> that cannot be accomplished by the self-assembled itinerary. Such replenishment is supposed to finish at the early time without increasing the time of CBD and concurrently causing the growth of the CdSe particles.

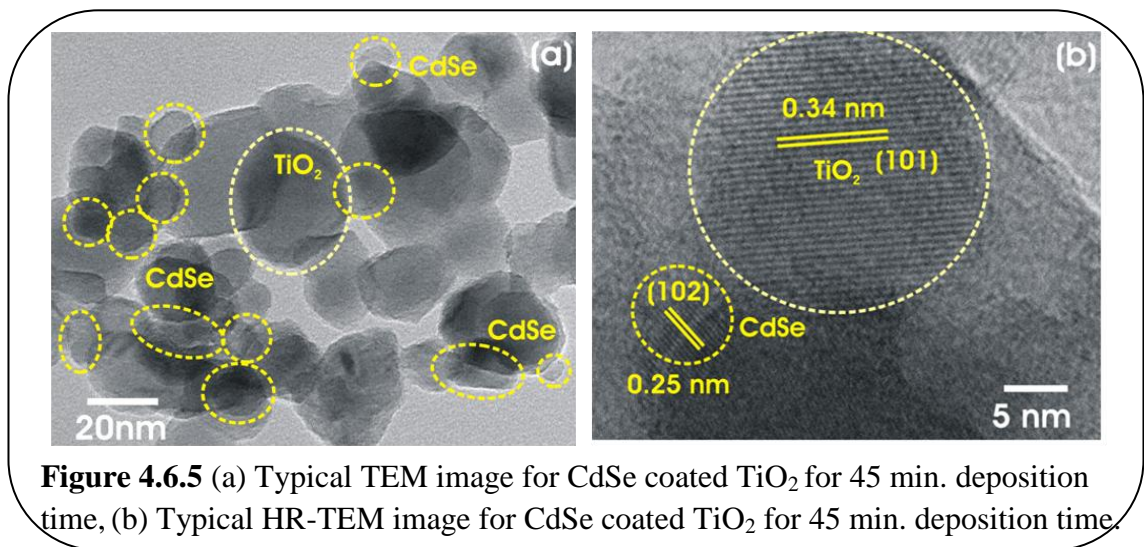
#### 4.6.4 Surface morphological studies



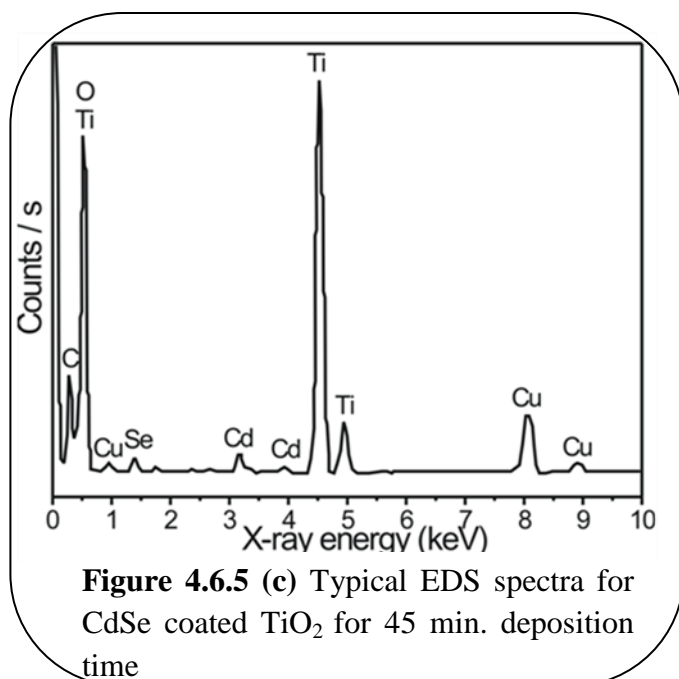
The surface morphology of TiO<sub>2</sub> electrode is shown in figure 3.6.4 (I) well explained in section 3.6.4 of chapter-III. For the clear understanding of the coating of CdSe layer, we have taken high magnified SEM images with the scale bar of 100 nm. Figure 4.6.4 (a-c) represents the surface morphologies of mesoporous TiO<sub>2</sub> film coated with CdSe nanoparticles thin film layers, synthesized at 45, 90 and 120 min. deposition times, respectively (150 min. deposited film is not shown). The small size of CdSe nanoparticles are evenly distributed encircling on the entire surface of the mesoporous TiO<sub>2</sub> film. The grain size observed is less than 10 nm for 45 min. deposited CdSe (figure 4.6.4 (a)) with well coverage. For 90 min. (figure 4.6.4 (b)) deposited film, total coverage of CdSe nanoparticles on the surface of TiO<sub>2</sub> is seen along with small overgrowth of CdSe. Figure 4.6.4 (C) reveals the morphology after 120 min. deposition time in which clear agglomeration of small size particles is

observed. It shows; the glossy surface of CdSe nanoparticles coverage on the TiO<sub>2</sub> filled in the gaps between TiO<sub>2</sub> as well. The essential point here is that SEM analysis does not tell about exact size and shape of CdSe grown on TiO<sub>2</sub> nanoparticles. Hence, for the determination exact size and shape of CdSe nanoparticles attachment on TiO<sub>2</sub> electrode; further TEM analysis is performed. The surface area measurement, we have followed the process explained in section 3.6.4 and calculated using equation 3.5 of chapter-III. The BET measurement of mesoporous TiO<sub>2</sub> film gives a surface area 56.42 m<sup>2</sup>/g. The CdSe coating on mesoporous film reduces the surface area of the film as depicted in the Table 4.2. The data is in well support to the observation from surface morphological studies.

#### 4.6.5 Size, shape, structure and elemental confirmation



In order to better understand the exact size, shape and structure of synthesized TiO<sub>2</sub>/CdSe layer nanostructures, we have performed the TEM and HR-TEM. Figure 4.6.5 (a) shows larger size TiO<sub>2</sub> (light yellow circles) with the size between 20-30 nm with small nanoparticles of CdSe with the size less than 10 nm (dark



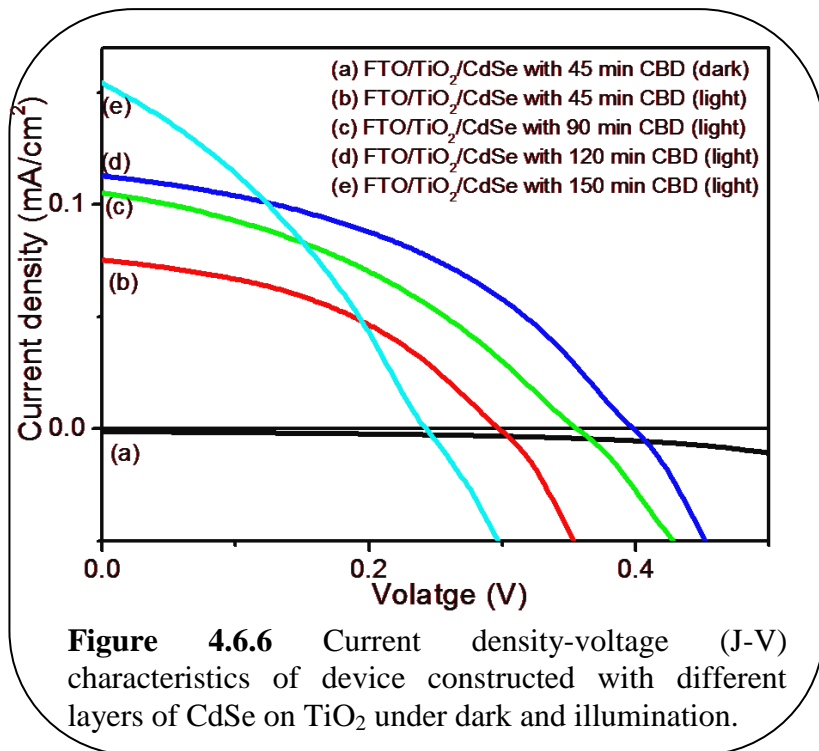
yellow circles). This is rather clear indication for the attachment of CdSe nanoparticles on TiO<sub>2</sub> which was accomplished by using simple chemical route at room temperature. In order to get in depth analysis of crystallographic structure of both CdSe and TiO<sub>2</sub>, many times ultra-sonication was done before placing the samples under investigation to get clear transmission images with the lattice fringes. The CdSe coated TiO<sub>2</sub> nanoparticles investigated with HR-TEM exhibit a crystallographic structure. Lattice fringes of a TiO<sub>2</sub> as well as for CdSe deposited for 45 min. is clearly visualized in Figure 4.6.5 (b). The lattice spacing measured for the crystalline along (101) plane is 0.34 nm, corresponding to the (101) plane of anatase TiO<sub>2</sub> (84-1285 and JCPDS 21-1272). The CdSe particle size is in the range of 4 to 5 nm for 45 min. deposited film with the inter planer spacing of 0.25 nm which is assigned to (102) plane of CdSe with hexagonal crystal structure and well supported by XRD studies.

The composition of the CdSe on TiO<sub>2</sub> was identified by using energy-dispersive X-ray spectroscopy (EDS) measurement, as shown in Figure 4.6.5 (c). The Cd, Ti and Se, O peaks are clearly observed in the EDS spectrum, whereas obtained Cu and C from the carbon coated copper grid. The quantitative analysis of the EDS spectrum gives a Cd:Se atomic ratio of about 1:1; indicating CdSe are likely to be stoichiometric. The result confirms that CdSe nanoparticles are successfully assembled on the surface of the TiO<sub>2</sub> film via low cost wet chemical techniques.

#### **4.6.6 Device fabrication and testing**

All the sandwich type device were constructed according to the procedure explained in section 3.6.6 (chapter-III) while performance of cell constructed with TiO<sub>2</sub> as a photoanode was explained in similar section and its J-V characteristics illustrated in figure 3.6.6 of chapter-III. Here, figure 4.6.6 shows the J-V (current density vs. voltage) curve measured under dark as well as in AM 1.5 illumination (50 mW/cm<sup>2</sup>) of light intensity. All cells constructed with TiO<sub>2</sub>/CdSe photoanode did not show any significant activity in the dark rather showed heterojunction properties and hence, as typical only dark curve for cell constructed with TiO<sub>2</sub>/CdSe (45 min. CBD) photoanode is illustrated and shown in figure 4.6.6 (a) as an example. The light illumination linearly enhances the current density along with the photovoltage on device constructed with 45 min. to 150 CBD deposited CdSe nanoparticles and are depicted in figure 4.6.6 (b-e). The enhancement clearly demonstrates the growth of CdSe layer on mesoporous TiO<sub>2</sub> film with increase in CBD deposition time; traps

more incoming incident light which is directly related with generation of photocurrent. The UV-Visible and surface morphological studies are in well supports; as the CdSe deposition time rises on TiO<sub>2</sub> electrode,



simultaneously surface area decreases of TiO<sub>2</sub> and increases internal surface area of CdSe for more absorptions of incident visible light. This enhancement in the optical absorption may be responsible for the improved photocurrent density under simulated sunlight and supported by optical studies.

The photovoltage generated in the semiconductor sensitizer solar cell is characteristics of the recombination centres. The increase in deposition time also increases number of recombination centres up to 120 min. CBD deposition time and decreases further for 150 min. CBD deposition, may be due increase in deposition time causes agglomeration of CdSe nanoparticles inside TiO<sub>2</sub> pores which restrict the penetration of a liquid electrolyte through the porous. This decreases electrolyte absorber layer contact. This is also responsible for the decreases in photovoltage.

However, for the maximum conversion light energy into electric energy requires appropriate thickness and higher absorption is required. And is combine property of photovoltage and photocurrent generated in the device. This condition is fulfill by the photoanode designed with 120 min. CBD deposition of CdSe. Hence, device constructed with 120 min. CdSe deposited gives maximum conversion efficiency 0.045%. The detailed photovoltaic parameters such as current density ( $J_{sc}$ ), open circuit voltage ( $V_{oc}$ ), fill factor (FF), power conversion efficiencies ( $\eta\%$ ) equation 3.6 (chapter III), series resistance ( $R_s$ ), shunt resistance ( $R_{sh}$ ) and flat band potential ( $V_{FB}$ ) are depicted in Table 4.2.

The J-V characteristics curves are also used to find electrical properties such as  $R_s$  and  $R_{sh}$ . The description of calculation of  $R_s$  and  $R_{sh}$  from J-V curves is given in section 3.6.6 of chapter-III. The  $R_s$  and  $R_{sh}$  were calculated from the J-V curves for all the constructed cells and are depicted in table 4.2. The result also matches with justification and the calculated  $R_s$  decreases with increase in deposition time i.e. thickness of the absorber layer. With increase in deposition time, the coating of TiO<sub>2</sub> surface simultaneously increases in layer heterostructure and this improves electron transportation in extremely thin film absorbing layer consisting of nanoparticles solar cell. This may be due to the increase in thickness of CdSe in layer heterostructures, simultaneously decreases the resistance of TiO<sub>2</sub> and increases the conductivity of materials.

The  $R_{sh}$  is affected by both charge carrier recombination and short circuiting within the cell. Therefore highly layer heterostructure electrodes can result into pin holes providing access to the FTO substrate and short circuiting, hence the  $R_{sh}$  will decrease. The calculated  $R_{sh}$  results shows that with increasing deposition i.e coating of the CdSe layer lowers down the participation of FTO layer by extremely thin film consisting of nanoparticles and increases the number of available recombination centres upto 120 min. CBD deposition of CdSe. While further increase in deposition time results into agglomerations of CdSe particles and reduce the electrolyte contact within absorber layer inside pores and reduces the recombination centres and decreases the  $R_{sh}$ . The calculated  $R_s$  and  $R_{sh}$  from J-V curves are tabulated in table 4.2.

The position of  $V_{FB}$  is equal to the photocurrent onset of the photoelectrode. The  $V_{FB}$  is an important factor in explaining charge transfer process across the semiconductor electrolyte junction of the PEC cell. The value of  $V_{FB}$  can be obtained by using Mott-Schottky relation equation 3.7 of chapter-III. An extrapolation of the Mott-Schottky plot to  $1/C^2 = 0$  yield the potential called  $V_{FB}$  which are tabulated in Table 4.2. The  $V_{FB}$  was found to be decreases with increasing thickness and reduces electrolyte contact with TiO<sub>2</sub>. Increase in capacitance with CdSe layer clearly indicates the reduction of voids, roughness, non-uniformity of the TiO<sub>2</sub> surface. The reduction in surface roughness of TiO<sub>2</sub> with CdSe coating is well supported by the surface morphological studies, whereas the agglomerations reduce the electrolyte contact with absorber layer inside pores. Hence decrease in the capacitance value with

more negative  $V_{FB}$  is observed for 150 min. deposited CdSe than 120 min. deposited CdSe.

**Table 4.2** Photovoltaic output parameters and surface area for CdSe as a sensitizer.

TiO <sub>2</sub> /CdSe CBD deposition time (min.)	$J_{sc}$ (mA. cm <sup>-2</sup> )	$V_{oc}$ (mV)	FF (%)	$\eta$ (%)	$R_s$ ( $\Omega$ . cm <sup>2</sup> )	$R_{sh}$ (k $\Omega$ . cm <sup>2</sup> )	$V_{FB}$ (V)	Surface area (m <sup>2</sup> g <sup>-1</sup> )
<b>45</b>	0.076	298	38.6	0.018	783	1.33	-0.70	19.31
<b>90</b>	0.105	355	39.3	0.029	642	1.53	-0.60	13.89
<b>120</b>	0.133	397	42.8	0.045	386	2.16	-0.38	10.40
<b>150</b>	0.157	240	35.3	0.027	339	1.16	-0.50	8.52

#### 4.7. Conclusions

1. We have successfully synthesized CdSe ETA layer consisting of nanoparticles by simple low cost CBD technique at room temperature onto TiO<sub>2</sub> without using linker/ligand molecules.
2. The size of CdSe nanoparticles in ETA layer is controlled by slow addition of Na<sub>2</sub>SeSO<sub>3</sub> and deposition time. The structural study indicates formation of anatase phase with tetragonal crystal structure of TiO<sub>2</sub> and hexagonal crystal structure for CdSe in layer heterostructure. Both XRD and HR-TEM results confirms the similar structure. Finally elemental analysis confirms the presence of both TiO<sub>2</sub> and CdSe in the layer heterostructure.
3. It is observed from SEM images that; porous TiO<sub>2</sub> provides high surface area to grow CdSe nanoparticles. The average grain size of TiO<sub>2</sub> ranges from 20-30 nm. With increasing deposition time, CdSe nanoparticles effectively cover the TiO<sub>2</sub> surface and finally effective agglomerations were seen over 120 min. deposited.
4. Finally, the synthesized layer heterostructure is used as a photoanode in sandwich type solar cell. In dark, all device shows heterojunction properties and their performance increases in light with increase in number of immersions and achieved 0.045% efficiency for 120 min. deposited CdSe films.
5. The photovoltaic parameters are well correlated with structural, optical absorption and surface morphological studies. As with increase in deposition time, particle size of the CdSe simultaneously increases and enhances the optical absorption with increase in thickness of CdSe in layer heterostructure.